IR and Raman characterization of the zincocenes (η5-C 5Me5)2Zn2 and (η5- C5Me5)(η1-C5Me5)Zn

ARTICLE *in* THE JOURNAL OF PHYSICAL CHEMISTRY A · OCTOBER 2008

Impact Factor: 2.69 · DOI: 10.1021/jp805291e · Source: PubMed

IR and Raman Characterization of the Zincocenes $(\eta^5\text{-}C_5Me_5)_2Zn_2$ and $(\eta^5\text{-}C_5Me_5)(\eta^1\text{-}C_5Me_5)Zn$

Diego del Rio,[†,#] Irene Resa,[†] Amor Rodriguez,[†] Luis Sánchez,[†] Ralf Köppe,*[,‡] Anthony J. Downs,*[,§] Christina Y. Tang,[§,†] and Ernesto Carmona*[,†]

Instituto de Investigaciones Químicas−Departamento de Química Inorgánica, Universidad de Sevilla-Consejo Superior de Investigaciones Científicas, Américo Vespucio 49, 41092 Sevilla, Spain, Institut für Anorganische Chemie, Universität Karlsruhe, Engesserstrasse 15, geb. 30.45, Karlsruhe 76128, Germany, and Inorganic Chemistry Laboratory, University of Oxford, South Parks Road, Oxford, OX1 3QR, U.K.

Received: June 12, 2008; Revised Manuscript Received: August 1, 2008

The measured Raman and IR spectra of solid, polycrystalline bis(pentamethylcyclopentadienyl)dizinc, $(\eta^5\text{-}C_5Me_5)_2Zn_2$, **1**, and bis(pentamethylcyclopentadienyl)monozinc, $(\eta^5\text{-}C_5Me_5)(\eta^1\text{-}C_5Me_5)Zn$, **8**, are reported in some detail. The IR spectra of the vapors of **1** and **8** each trapped in a solid Ar matrix at 12 K confirm the essentially molecular character of the solids. The experimental results have been interpreted with particular reference (i) to the corresponding spectra of ^{68}Zn-enriched samples of the compounds, and (ii) to the spectra simulated by density functional theory (DFT) calculations at the B3LYP level. The marked differences of structure of **1** and **8** contrast with the relatively close similarity of their vibrational spectra, disparities being revealed only on detailed scrutiny, including the effects of ^{68}Zn enrichment, and primarily at wavenumbers below 1000 cm^{-1}. The Zn−Zn stretching motion of **1** features not as a single, well-defined mode identifiable with intense Raman scattering but in several normal modes which respond in varying degrees to ^{68}Zn substitution. A stretching force constant of 1.42 mdyne Å^{-1} has been estimated for the Zn−Zn bond of **1**.

1. Introduction

The recent synthesis and characterization of bis(η^5-pentamethylcyclopentadienyl)dizinc, $(\eta^5\text{-}C_5Me_5)_2Zn_2$, **1**,[1] made a landmark in group 12 chemistry by affording the first example of a molecular compound featuring a Zn−Zn bond. Its identification has attracted considerable attention in the scientific community[2] and was closely followed by a flurry of theoretical treatments seeking to explain its structure and bonding.[3,4] Subsequent experimental studies have led very recently[5] to the synthesis of a second example of a dizincocene in $(\eta^5\text{-}C_5Me_4Et)_2Zn_2$. The first report of **1** also stimulated the search for further examples of Zn−Zn-bonded compounds. Hot on the heels of **1** came the synthesis of $[HC(MeCNAr)_2]_2Zn_2$, **2**, where Ar = 2,6-^{i}Pr$_2$C$_6$H$_3$, reported by Wang et al.;[6] coordination of the bidentate β-diketiminate ligands gives threefold coordination at the Zn atoms for the metal−metal bond. Structures similar to that of **2** have been reported for the compound $[dpp\text{-}Bian]_2Zn_2$, **3**, where $[dpp\text{-}Bian]^{\bullet-}$ is the radical monoanion of 1,2-bis[(2,6-diisopropylphenyl)imine]acenaphthene,[7] and for the dianions $[\{\eta^2\text{-}(NAr)_2C_2Me_2\}_2Zn_2]^{2-}$, **4**,[8] and $[\{\eta^2\text{-}(NAr)_2SiMe_2\}_2Zn_2]^{2-}$, **5**,[9] both containing bidentate, sterically encumbered diamido ligands (Ar = 2,6-^{i}Pr$_2$C$_6$H$_3$) and which have been isolated as their $[Na(THF)_2]^+$ and K^+ salts, respectively. A rather different zinc−zinc-bonded compound Ar'_2Zn_2 featuring the very bulky terphenyl ligand Ar′ = C$_6$H$_3$-2,6-(C$_6$H$_3$-2,6-^{i}Pr$_2$)$_2$ and two-coordinated metal atoms, **6**, was reported in 2006 by Power and co-workers.[10] The same researchers have also described an unusual hydride and Na^+-bridged Zn−Zn-bonded complex $Ar'_2(\mu\text{-}H)(\mu\text{-}Na)Zn_2$, as well as the Cd and Hg analogues of **6**.[10] The Zn−Zn bond distance in these various compounds ranges from 2.305(3) Å in **1**[1,5] to 2.3994(6) Å in **5**.[9] In evidence of the interest and activity in this general area of main group dimetal compounds we may also cite the very recent characterization of the Mg−Mg-bonded compounds Mg_2L_2, where L = $[ArNC(N^iPr_2)NAr]^-$ and $[\{ArNC(Me)\}_2CH]^-$ (Ar = 2,6-^{i}Pr$_2$C$_6$H$_3$), that feature Mg−Mg bonds measuring ca. 2.85 Å.[11]

Dizinc compounds of this sort, which are usually formed by reduction of a suitable zinc(II) precursor, cannot entirely escape uncertainty. Whatever circumstantial evidence may suggest, the difference between an unsupported Zn−Zn bond in a compound of the type LZnZnL and a hydrogen-bridged unit in $LZn(\mu\text{-}H)_2ZnL$ [i.e., a dimer of the appropriate zinc(II) hydride] is less than easy to establish. With X-ray diffraction as the arbiter of the crystal structures, it is inevitably difficult to locate H atoms in close proximity to the heavily scattering metal atoms. Neutron diffraction studies have been undertaken, and while being in accord with the X-ray structural analysis, they do not settle the issue.[12] Little is known about zinc(II) hydrides at large; thermal lability, combined with a marked tendency to oligomerize or polymerize, has resulted in a comparative dearth of well-characterized, stable species.[10,13] It is interesting, though, that Power and his group have described the preparation of the compound $Ar'Zn(\mu\text{-}H)_2ZnAr'$, where Ar′ = C$_6H_3$-2,6-(C$_6H_3$-2,6-^{i}Pr$_2$)$_2$, **7**.[10] In this case, the Zn···Zn distance measures 2.4084(3) Å, making it 0.049 Å longer than in **6**, but still not very different from the longest Zn−Zn bond length reported to date. Characterization of a hydride derivative related to **2**, viz., $RZn(\mu\text{-}H)_2ZnR$, where R = HC(MeCNC$_6$H$_3$-2,6-^{i}Pr$_2$)$_2$, however, reveals a Zn···Zn distance of 2.4513(9) Å,[14] nearly 0.10 Å longer than the Zn−Zn bond length in **2**.

* To whom correspondence should be addressed. E-mail: ralf.koeppe@chemie.uni-karlsruhe.de (R.K.); tony.downs@chem.ox.ac.uk (A.J.D.); guzman@gus.es (E.C.).
† Universidad de Sevilla-Consejo Superior de Investigaciones Científicas.
‡ Universität Karlsruhe.
§ University of Oxford.
# Current address: SRI International, 333 Ravenswood Avenue, Menlo Park, CA 94025.

10.1021/jp805291e CCC: $40.75
Published on Web 09/27/2008

Spectroscopic measurements have so far played a distinctly limited part in the characterization of the new dizinc compounds, LZnZnL, being confined mainly to confirming the presence and mode of coordination of the ligands L. The relative complexity of these ligands, which typically display rich vibrational and NMR spectra, restricts the usefulness of such spectra for diagnostic purposes. Thus, the normal evidence of a fragment such as $Zn(\mu\text{-}H)_2Zn$ that an IR or Raman spectrum might be expected to provide[13] is liable to be masked by the many absorptions or emissions arising from the internal vibrations of the two L ligands. On the other hand, the large Raman scattering cross section associated with the $\nu(Zn-Zn)$ vibration would normally be expected to reveal itself as an intense signal at low wavenumber. Indeed, Raman spectroscopy has a long history of providing cogent and distinctive evidence for the presence of metal−metal bonds,[15] as exemplified by the cases of $Hg_2^{2+}(aq)$,[16] Cd_2^{2+},[17] Ga_2,[18] and $[Ga_2X_6]^{2-}$ (X = Cl, Br, or I).[19]

Despite the increasing number of claims to compounds containing the $[Zn-Zn]^{2+}$ core, little has been made of their vibrational spectra. To date, the only evidence of a $\nu(Zn-Zn)$ mode came 40 years ago with the investigation of $Zn/ZnCl_2$ glasses, Raman scattering at 175 cm^{-1} being attributed to $\nu(Zn-Zn)$ of a Zn_2^{2+} unit.[20] Two of the theoretical studies of **1** have included calculations of the main features of the IR and Raman spectra,[4a,b] but these have yet to be validated by experimental data.

Here we describe the IR and Raman spectra of polycrystalline $(\eta^5\text{-}C_5Me_5)_2Zn_2$, **1**, and compare them with the corresponding spectra of the monozincocene $(C_5Me_5)_2Zn$, **8**, the crystal structure[21] and gas electron diffraction pattern[22] of which signal the formulation $(\eta^5\text{-}C_5Me_5)(\eta^1\text{-}C_5Me_5)Zn$. It is noteworthy that a similar unsymmetrical, slipped-sandwich structure has been determined very recently[23] for the isoelectronic $[(C_5Me_5)_2Ga]^+$ cation isolated as its tetrafluoroborate salt, whereas the corresponding $[(C_5Me_5)_2Al]^+$ cation has a symmetrical $[(\eta^5\text{-}C_5Me_5)_2Al]^+$ structure as characterized in its tetrachloroaluminate salt. As part of the present study, we have also measured the IR spectra of **1** and **8** each isolated in a solid Ar matrix at 12 K. The interpretation of the spectra has been aided by reference (i) to the spectra of ^{68}Zn-enriched samples of **1** and **8** and (ii) to the spectra forecast by density functional theory (DFT) calculations at the B3LYP level. In fact, **1** and **8** exhibit vibrational spectra that are remarkably similar in many ways. Differences become apparent only on detailed scrutiny of the regions of the spectra at wavenumbers below 1000 cm^{-1}. The Zn−Zn stretching motion manifests itself not in a single, well-defined normal mode identifiable with intense Raman scattering, but in several normal modes which respond in varying degrees to ^{68}Zn substitution.

2. Experimental and Computational Details

2.a. Synthesis. Samples of **1** and **8** containing isotopically natural Zn were prepared by the methods described previously.[1,5,22] ^{68}Zn-labeled samples were prepared from a commercial sample of ^{68}ZnO (Trace Sciences International Corp., Ontario, Canada; ≥99% enrichment) which was converted to $^{68}ZnCl_2$ as the starting material.[5] All the syntheses and manipulations were carried out under oxygen-free argon using conventional Schlenk and glovebox techniques. Solvents were rigorously dried and degassed before use. Samples were purified by repeated crystallization from pentane or diethyl ether at −20 °C (at least twice), and their purity was checked by ^1H and $^{13}C\{^1H\}$NMR measurements.

2.b. Spectroscopic Measurements. Raman spectra of polycrystalline samples of **1** and **8** were measured initially at Oxford using a Dilor Labram 14/231 M spectrometer having a CCD detector, a He−Ne laser providing excitation at 632.8 nm. Superior, but otherwise similar, results were subsequently obtained at Karlsruhe with the aid of a Dilor XY800 spectrometer equipped with two premonochromators and a spectrograph, and a CCD camera (Wright Instruments) as detector. The 488.0 nm line of an Ar^+ ion laser (Coherent, Innova 90-5) afforded the means of excitation. Spectra were recorded with a resolution of 1.5 cm^{-1}.

IR spectra for solid **1** and **8** in the form of Nujol mulls pressed between CsI windows were recorded in the range of 4000−200 cm^{-1} in Seville using a Perkin-Elmer 883 spectrometer. The essential details of these spectra were later confirmed by measurements made in Karlsruhe on disks of the compounds dispersed in CsI that had been rigorously predried by melting under vacuum; these involved the use of a Bruker 113v instrument.

Samples of **1** and **8** were vaporized severally at 325 K and 341−358 K, respectively, and the vapor of each was quenched with an excess of Ar on the face of a highly polished copper block at 12 K to give solid matrixes which were interrogated by IR measurements made in reflection with the Bruker 113v spectrometer. The matrix apparatus has been described elsewhere.[24] Much trial and error was needed to secure the optimum conditions for the vaporization of **1**, and in these circumstances it was not feasible to carry out similar experiments with the ^{68}Zn-enriched compound. In no case was it possible to achieve vaporization without some decomposition to **8**, and careful analysis of the spectra of the matrixes prepared under different conditions was needed in order to distinguish the absorptions due to **1** from those due to **8**. Similar observations had been made during high-resolution mass spectrometric studies of **1**.[5] Close attention to the growth patterns of the bands, aided by comparison with the spectra of **1** and **8** supported as CsI disks and of the vapor of **8** isolated in a solid Ar matrix, led ultimately to the confident identification of 11 IR transitions that could be attributed to matrix-isolated molecules of **1**. The sharpness of the absorptions compared with those of the solid compound testified that the molecules were indeed well isolated, although there was no other radical difference between the two spectra.

The matrixes doped with **1** showed signs of discoloration associated presumably with partial decomposition, and this, allied to the low concentration of **1**, defeated all attempts to measure a Raman spectrum. Speculative experiments were also performed to test the effects of broad-band UV−vis irradiation on matrix-isolated samples of **1**, but the IR spectrum showed no significant change. Some photoactivity, at least under UV irradiation, might be expected, and it is likely that the matrix cages confining the molecules of **1** prevent the separation of what would be relatively large photofragments, e.g., $C_5Me_5Zn^{\bullet}$, and simply result in recombination.

Vaporization of **8** was less problematic than that of **1**, and IR spectra were recorded for matrix-isolated samples of both the isotopically natural and ^{68}Zn-enriched compound. Analysis of these spectra was complicated, however, by the appearance of weak bands due not only to regular impurities such as CO_2 but also to traces of the organic solvent used for the preparation and purification of the compound. Appropriate care was needed therefore in identifying the transitions properly belonging to **8**.

2.c. Quantum Chemical Calculations. The geometries of $(\eta^5\text{-}C_5Me_5)_2Zn_2$, **1**, and $(C_5Me_5)_2Zn$, **8**, were computed under D_{5h} symmetry in the first case and with no symmetry constraints in the second. The calculations were carried out within the framework of DFT at the B3LYP hybrid level,[25] using a

6-311+G** basis set for each atom. Vibrational frequency calculations were performed on the optimized structures at this level of theory by diagonalization of the analytically computed Hessian. For **1** a small imaginary frequency (13i cm^{-1}) was found. The associated mode did not, however, involve movement of the Zn atoms, and so the optimized structure and other computed vibrational details were used in the ensuing discussion. All these calculations entailed the use of the Gaussian03 package.[26] Simulated IR and Raman spectra were produced with the aid of the SWizard program, revision 4.2[27] using the Gaussian model. The half-bandwidths, $\Delta_{1/2,I}$, were taken for the purposes of reproducing the spectra of the solids to be 15 cm^{-1}. Figures and depictions of selected vibrational modes have been generated using DIAMOND and MOLDEN.[28]

Both the structure and vibrational force field of **1** with D_{5h} symmetry were also calculated using the TURBOMOLE program package.[29] Here the density functional calculations were performed with the B3LYP Gaussian.[30,31] The numerical integration was carried out with the aid of the m^3 grid. With 6-311+G** basis sets employed for all atoms, the force constant matrix in the basis system of Cartesian coordinates was calculated by numerical second derivation of the energy using the module NumForce. The modules RELAX[30] and AOFORCE[32] afforded the means of transforming this force constant matrix into a system of symmetry coordinates, and then of extracting the potential energy distributions of the fundamentals contained by the a_1' and a_2'' irreducible representations.

3. Results and Discussion

3.a. Experimental Findings. The Raman and IR spectra of polycrystalline $(\eta^5\text{-}C_5Me_5)_2Zn_2$, **1**, are illustrated in Figure 1, and the wavenumbers and relative intensities of the features are detailed in Table 1. Figure 2 depicts the IR spectrum of matrix-isolated **1**, the relevant details being included in Table 1. The corresponding spectra of polycrystalline $(\eta^5\text{-}C_5Me_5)(\eta^1\text{-}C_5Me_5)Zn$, **8**, are illustrated in Figure 3, with the wavenumbers and relative intensities set out in Table 2. As is to be expected, the spectra of ^{68}Zn-enriched samples of **1** and **8** mirror very closely those of isotopically natural samples (^{64}Zn 48%, ^{66}Zn 28%, ^{67}Zn 4%, and ^{68}Zn 19%),[33] though with evidence of slight but significant changes of contour, as well as perceptible wavenumber shifts, on the part of some bands. The magnitudes of these shifts are included in Tables 1 and 2.

At wavenumbers greater than 1000 cm^{-1}, the IR and Raman spectra of solid **1** show an obvious affinity to those of decamethylferrocene, $(\eta^5\text{-}C_5Me_5)_2Fe$.[34] This region is dominated by vibrational modes which are confined mainly to internal motions of the $\eta^5\text{-}C_5Me_5$ ligands. The most prominent features in both the IR and the Raman spectra, observed at wavenumbers near (i) 2900 and (ii) 1400 cm^{-1}, are then attributable to what are (i) substantially ν(C−H) and (ii) complicated modes which, on the evidence of subsequent analysis as well as earlier studies,[4] approximate mainly to breathing vibrations of the C_5Me_5 ligands.

It is in the region 1000−2000 cm^{-1} that signs of the stretching vibrations of a dihydrido-bridged Zn(μ-H)$_2$Zn might be expected to appear.[13,35] Unfortunately, the recent reports of the compounds RZn(μ-H)$_2$ZnR with R = C_6H_3-2,6-(C_6H_3-2,6-^{i}Pr$_2$)$_2$[10] and HC(MeCNC_6H_3-2,6-^{i}Pr$_2$)$_2$[14] make no mention of their vibrational spectra. Theoretical calculations on the dimer HZn(μ-H)$_2$ZnH forecast that the stretching vibrations of the central Zn(μ-H)$_2$Zn core appear at wavenumbers between 1200 and 1600 cm^{-1}.[36] In the case of the gallium hydrides $H_2Ga(\mu\text{-}H)_2GaH_2$[37] and $Me_2Ga(\mu\text{-}H)_2GaMe_2$,[38] the corresponding M(μ-H)$_2$M vibrations

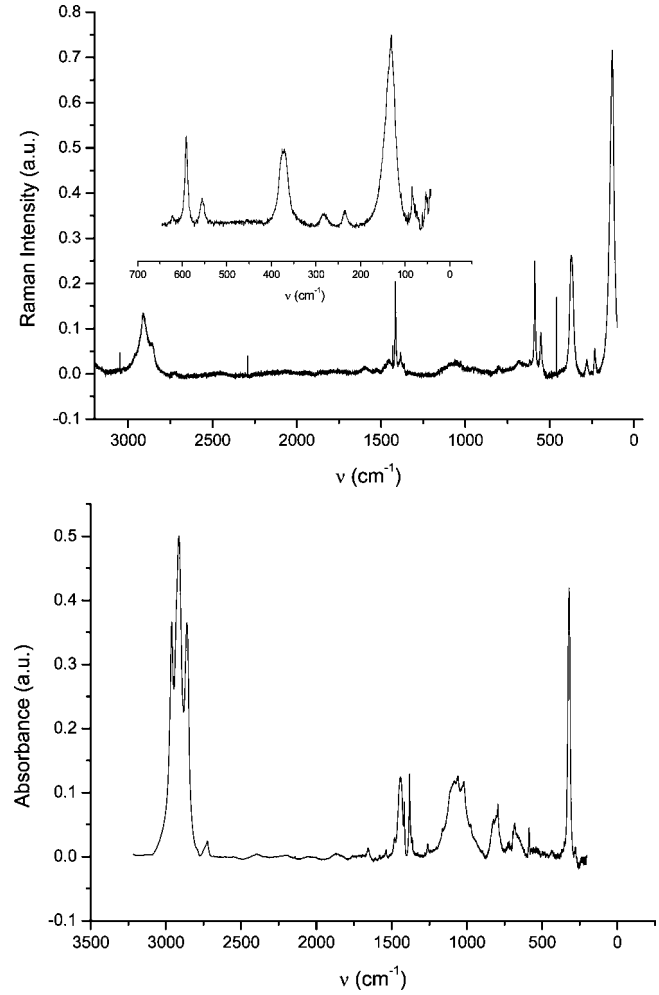

Figure 1. Measured Raman spectrum (30−3200 cm^{-1}, excited at λ = 488.0 nm) and IR spectrum (200−3500 cm^{-1}) of isotopically natural samples of polycrystalline bis(pentamethylcyclopentadienyl)dizinc, $(\eta^5\text{-}C_5Me_5)_2Zn_2$, **1**.

are responsible for prominent IR absorptions and Raman emissions at wavenumbers between 1150 and 1500 cm^{-1}. Although such features may be obscured, there was no suggestion of any bands in the vibrational spectra of **1** that could not be accounted for by vibrational modes localized mainly in the C_5Me_5 ligands.

Only at wavenumbers below 1000 cm^{-1} is the influence of the Zn_2, Zn, or Fe core expected to become apparent. The most intense IR absorption of $(\eta^5\text{-}C_5Me_5)_2Fe$ in this region, occurring at 455 cm^{-1}, has been attributed to what is primarily the antisymmetric metal···ring stretching vibration.[34] By contrast, the most intense IR absorption of solid **1** occurs at 320.6 cm^{-1}. The most intense Raman scattering of $(\eta^5\text{-}C_5Me_5)_2Fe$ appears at 590 and 378 cm^{-1}.[34] The first feature has been associated with a perpendicular ring deformation and the second with either a symmetric ring tilting or the symmetric metal···ring stretching vibration. The Raman spectrum of **1** resembles that of $(\eta^5\text{-}C_5Me_5)_2Fe$ in its display of strong scattering at 590.8 and 373.6 cm^{-1} but appears to differ in displaying even stronger scattering at 130.7 cm^{-1} to which no counterpart has been reported for decamethylferrocene. In the light of the intensity of this last feature, we were tempted initially to conclude that it represents in large part a ν(Zn−Zn) motion. Support for such a conclusion comes from the claim that the mode of Zn_2Cl_2 believed most closely to approximate to ν(Zn−Zn) occurs at 175 cm^{-1}.[20] In other respects, we note a distinct lack of coincidences between

TABLE 1: Vibrational Spectrum of $Zn_2Cp^*_2$[a]

$Zn_2Cp^*_2$ solid		$Zn_2Cp^*_2$ CsI pellet		$Zn_2Cp^*_2$ Ar matrix	
Raman		infrared		infrared	
ν [cm^{-1}]	I	ν [cm^{-1}]	I	ν [cm^{-1}]	I
2914.1	vs	2962.1	vs		
		2915.8	vs	2918.3	s
2871.3	s, sh	2861.4	vs	2872.0	s
		2725.0	w, br		
		1658.9	w, br		
				1489.3	m
1462.9	m	1441.0	s	1457.9	vs
1418.1	vs	1416.0	?	1434.8	vs
1386.7	m	1380.8	s	1386.1	s
		1261.2	m		
1080	m, br	1083.3	s		
1029.7	w	1021.1	sh	1025.0	m
798.7	w	794.5	m	795.0	m
				740.0	m
		683.6	?	684.6	w
622.2	w				
590.8 (−1.8)	vs	586.8 (+0.9)	w		
555.1 (−0.5)	m				
373.6 (−4.2)	vs				
		320.6 (−1.9)	vs	329.3	vs
281.3 (−1.2)	m	278.6	w		
236.0 (−3.6)	m				
130.7 (0.0)	vs				
84.6	m				
52.9	m				

[a] Wavenumber shifts (in cm^{-1}) for the change from isotopically natural $Zn_2Cp^*_2$ to $^{68}Zn_2Cp^*_2$ are given in parentheses. The wavenumber accuracy is judged to be generally about ±1 cm^{-1}. Intensities: s strong, m medium, w weak, v very, sh shoulder, and br broad.

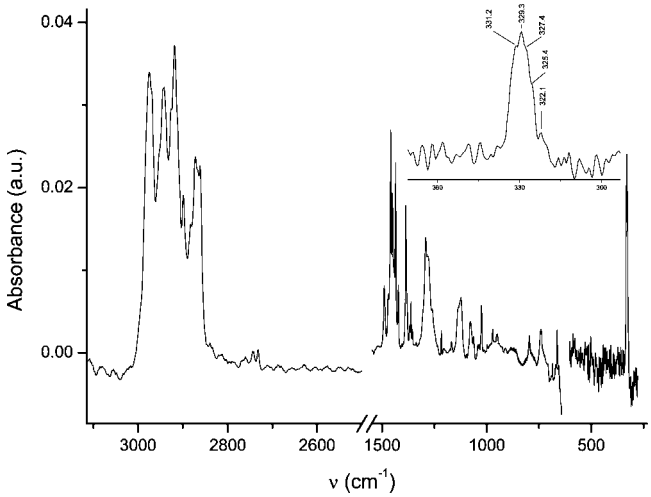

Figure 2. Measured IR spectrum (250−3100 cm^{-1}) of the vapor of **1** isolated in a solid Ar matrix at 12 K.

the IR and Raman features of **1** at wavenumbers below 1000 cm^{-1}, in keeping with the selection rules appropriate to a molecular skeleton of relatively high symmetry (D_{5h} on the evidence of the crystal structure[1,5]).

As noted in the Experimental and Computational Details section, analysis of the IR spectrum of **1** isolated in a solid Ar matrix at 12 K was complicated by partial decomposition of **1** to **8**. Allowance had also to be made for the presence of traces of unavoidable impurities (CO_2, CO, and H_2O). The combination of these impurities and **8** meant that some parts of the IR spectrum of **1** were obscured. By taking into account the spectra of solid **1** and **8** and of matrix-isolated **8** and also the IR

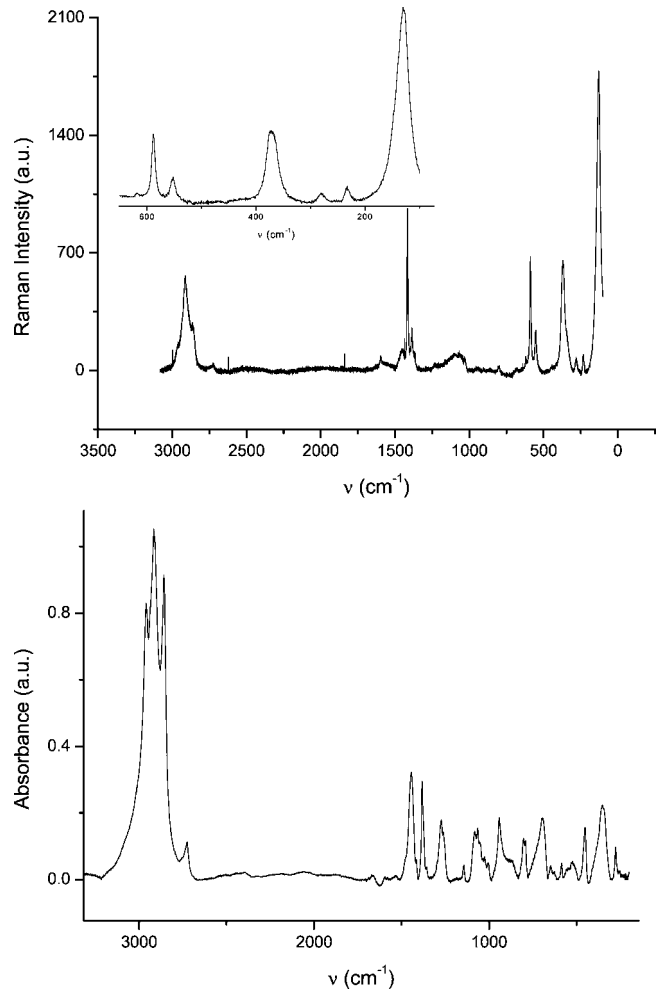

Figure 3. Measured Raman spectrum (100−3100 cm^{-1}, excited at λ = 488.0 nm) and IR spectrum (200−3200 cm^{-1}) of isotopically natural samples of polycrystalline bis(pentamethylcyclopentadienyl)monozinc, (η^5-C_5Me_5)(η^1-C_5Me_5)Zn, **8**.

spectrum simulated for **1** (q.v.), however, we have been able with some confidence to identify the absorptions listed in Table 1 with matrix-isolated **1**. Comparison of the resulting spectrum with that of solid **1** finds no significant change in the pattern of the bands and only minor changes of wavenumber. There is the expected sharpening of the bands as the molecule passes from the solid to the matrix-isolated state, with the result that more detail is discernible in some parts of the spectrum (e.g., 1400−1500 cm^{-1}). Generally speaking, though, the results of the matrix experiments confirm the crystallographic findings in their implication that the (η^5-C_5Me_5)$_2Zn_2$ molecules are not exposed to any unusual intermolecular interactions in the crystalline state.

The very different mode of coordination adopted by one of the C_5Me_5 ligands in **8**, i.e., (η^5-C_5Me_5)(η^1-C_5Me_5)Zn,[21] would be expected to give rise to IR and Raman spectra significantly different from those of **1**. As noted earlier, the IR spectrum of matrix-isolated **8** labored under the disadvantage of several weak absorptions, e.g., at 950−1200 cm^{-1}, due to traces of organic solvent. The Raman spectrum of parts of the solid also included a band at 254.6 cm^{-1}. This probably originates in traces of the $ZnCl_2$ starting material, which has a scattering cross section about 2 orders of magnitude greater than that of **8**.[39] Nevertheless, with due allowance for such potentially deceptive, albeit weak features, nearly all the Raman and IR bands listed in Table 2 belong, we believe, to **8**. Common features are of course to

TABLE 2: Vibrational Spectrum of $ZnCp^*_2$[a]

$ZnCp^*_2$ solid		$ZnCp^*_2$ CsI pellet		$ZnCp^*_2$ Ar matrix		$^{68}ZnCp^*_2$ Ar matrix	
Raman		infrared		infrared		infrared	
ν [cm^{-1}]	I	ν [cm^{-1}]	I	ν [cm^{-1}]	I	ν [cm^{-1}]	I
				2979	vs	2977.1	vs
		2959.7	vs	2969.4	vs	2968.9	vs
						2937.5	vs
				2927.0	vs	2926.5	vs
2913.3	vs	2915.8	vs				
				2881.6	s	2882.6	s
2860.0	s, sh	2858.0	vs	2861.4	vs	2860.4	vs
						2744.7	m
2727	w	2725.4	w				
1596.2	w, br (?)						
1532.1	w, br (?)						
						1484.4	w
				1464.2	m	1462.2	m
1450.8	m, br	1444.9	s	1450.2	vs	1450.2	vs
				1441.0	vs	1440.6	vs
1416.9	vs						
				1390.4	m	1390.4	m
1386.6	s	1383.2	s	1382.2	s	1382.2	s
		1274.2	m			1264.6	s, br
		1144.5	w			1141.2	w
		1084.3	m				
1048.5	m, br	1056.0	m	1059.6	m	1059.2	m
		1053	m, sh	1054.4	m, sh		
		1026.4	w	1033.2	m	1033.7	m
		1005.2	w			1013.4	w
		941.6	m			940.1	m
805.2	w, br	803.7	m				
		793.6	m				
		697.1	s			696.7	m
685.4	w, br			684.6	s	684.6	s
618.3	w	649.4	m				
588.3 (+0.3)	vs	585.8	w				
		523.6	w				
		451.7	m				
368.0 (+0.9)	s	352.9	s				
279.6 (+0.6)	m	277.2	w				
232.1 (−0.2)	m						
128.7 (+0.2)	vs						
79.7	w						

[a] Wavenumber shifts (in cm^{-1}) for the change from isotopically natural $ZnCp^*_2$ to $^{68}ZnCp^*_2$ are given in parentheses. The wavenumber accuracy is judged to be generally about ±1 cm^{-1}. Intensities: s strong, m medium, w weak, v very, sh shoulder, and br broad.

be found in the spectra of **1** and **8** at wavenumbers exceeding 1000 cm^{-1} where the vibrations are localized mainly in the ligands, but numerous differences of detail are also apparent, as in the regions 900−1100 and 400−700 cm^{-1} of the IR spectra or 600−900 cm^{-1} of the Raman spectra. What came as a particular surprise, however, was the discovery of how closely the Raman spectrum of **8** resembles that of **1** and, particularly, at wavenumbers below 600 cm^{-1}. Most notably, the intense Raman signals of **1** at 590.8, 373.6, and 130.7 cm^{-1} are matched by equally prominent signals of **8** at 588.3, 368.0, and 128.7 cm^{-1}. There must be serious doubts, therefore, about the attribution of the 130.7 cm^{-1} feature of **1** to a vibrational mode including a major ν(Zn−Zn) component.

In an attempt to gain a clearer understanding of the spectra, we have measured the spectra of ^{68}Zn-enriched samples of both **1** and **8** to seek evidence of changes in wavenumber and/or contour identifying any vibrational modes that entail significant motion of the metal atom or atoms. The Raman spectrum of solid **1** showed that replacement of the natural isotopic mix of Zn isotopes by ^{68}Zn led to wavenumber shifts of −1.8, −0.5, −4.2, −1.2, and −3.6 cm^{-1} by the bands originally centered at 590.8, 555.1, 373.6, 281.3, and 236.0 cm^{-1}, respectively. Yet the intense scattering at 130.7 cm^{-1} suffered no measurable shift (see Figure 4). Hence it appears that Zn−Zn stretching is not confined to a single well-defined vibrational mode and makes, at best, only a modest contribution to the mode responsible for the 130.7 cm^{-1} transition. The IR spectrum of solid **1** suffered little change on ^{68}Zn enrichment beyond a shift of −1.9 cm^{-1} on the part of the intense absorption originally centered at 320.6 cm^{-1}. ^{68}Zn enrichment of **8** resulted in apparent shifts of only −1.2, +0.9, and +0.6 cm^{-1} for the Raman bands at 554.1, 368.0, and 279.6 cm^{-1}, respectively, lying at or beyond the margins of significance in the context of the present measurements; no discernible shifts could be detected in any of the IR absorptions.

With the interpretation of the spectra, however, little further progress can be made in the absence of vibrational force fields appropriate to the molecules of **1** and **8**. In the following section we describe the results of DFT calculations designed to model such force fields.

3.b. Quantum Chemical Calculations. The structures of the molecules **1** and **8** were optimized at the B3LYP level of theory using 6-311+G** basis sets for all the atoms. Although a good description of the structures of both molecules can be achieved

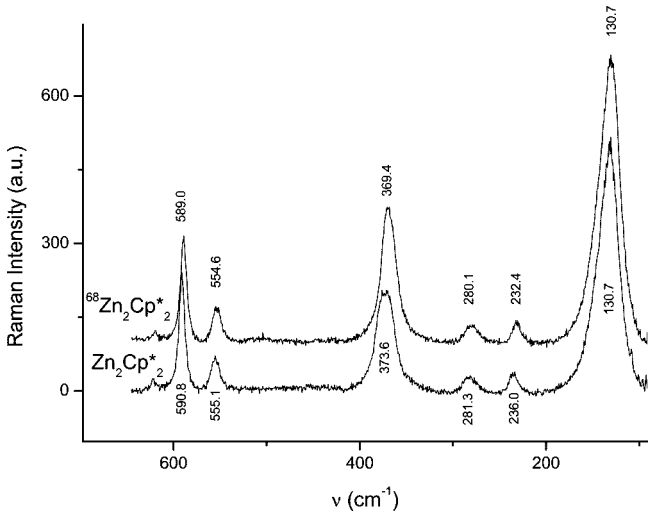

Figure 4. Comparison of the Raman spectrum of solid isotopically natural (η^5-$C_5Me_5)_2Zn_2$, **1**, with that of solid (η^5-$C_5Me_5)_2{}^{68}Zn_2$, **1**-^{68}Zn, in the region of 100−650 cm^{-1}.

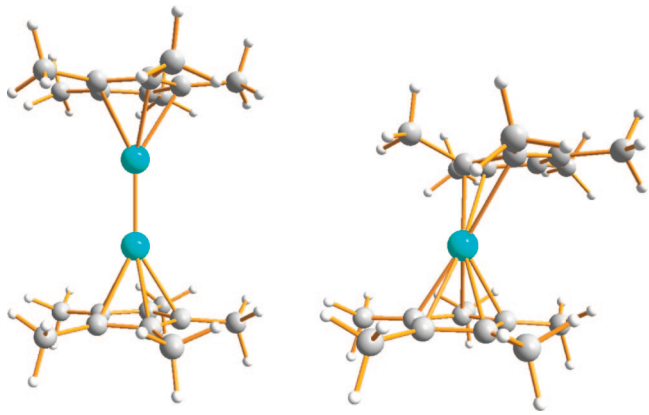

Figure 5. Optimized structures of the molecules of **1** and **8** calculated at the B3LYP level of theory using 6-311+G** basis sets for all atoms.

without the inclusion of diffuse functions, we found the use of such functions to be necessary for a realistic simulation of the IR and Raman spectra. Figure 5 shows the optimized structures calculated for **1** and **8** at this level of theory.

The geometry of **1** was optimized under the assumption of D_{5h} symmetry. The calculated Zn−Zn distance of 2.338 Å compares well with the value of 2.331 Å calculated at the B3LYP/6-311G* level of theory by the Seville group[5] and is also in satisfactory agreement with the experimental value of 2.305(3) Å found by X-ray diffraction studies of a single crystal at low temperature.[1,5] Each of the C_5Me_5 rings is coordinated in an η^5-fashion to either end of the Zn_2 unit lying along the C_5 axis, with a calculated Zn···C_{ring} distance of 2.313 Å. This estimate compares well with the narrow range of 2.27−2.30 Å determined experimentally.[1,5]

The calculated structure of **8** is characterized by one η^5-C_5Me_5 and a slipped η^1-C_5Me_5 ring. Zn···C_{ring} distances of the (η^5-C_5Me_5)Zn fragment range between 2.26 and 2.32 Å, whereas the Zn−C distance for the (η^1-C_5Me_5)Zn fragment is estimated to be 2.02 Å [cf., 2.09−2.30 and 2.09 Å, respectively, for (η^5-C_5Me_4Ph)(η^1-C_5Me_4Ph)Zn].[21] The calculated Zn−C−CH_3 angle of 101.4° is characteristic of the slipped structure and compares favorably with the experimental value of 106.7° [for $(C_5Me_4Ph)_2Zn$].[21]

Of the numerous theoretical studies on **1** that have been carried out so far, only two[4] have sought to simulate the main features of its IR and Raman spectra. Both have used DFT methods, with particular interest in the vibrational transitions that involve significant motion of the Zn atoms. Although there are some differences in the results and their interpretation, both these earlier studies seem to be agreed that no single mode can be identified with the Zn−Zn stretching vibration. On the other hand, there has been no previous opportunity to discover how well theory matches experiment. Our calculations of the vibrational properties of **1** have been designed not only for collation with the measured spectra of this compound but also for whatever contrast may be found with the simulated and measured spectra of the monozinc compound **8**.

As subjects for detailed vibrational analysis, both **1** and **8** present formidable problems. With 52 atoms and 150 normal modes of vibration, many of them of a complicated nature, **1** does have the advantage of D_{5h} symmetry, which implies the vibrational representation $10a_1' + 6a_1'' + 5a_2' + 9a_2'' + 15e_1' + 15e_1'' + 15e_2' + 15e_2''$. Operation of the selection rules at a purely molecular level then leads to the expectation of 40 Raman-active transitions ($10a_1' + 15e_1'' + 15e_2'$) and 24 IR-active ones ($9a_2'' + 15e_1'$), with mutual exclusion between Raman scattering and IR absorption. **8** may have one atom fewer than **1**, but its 147 normal modes do not enjoy the benefit of a significant degree of symmetry (C_s at best), and so the vibrational properties are even less amenable than are those of **1** to simple description in terms of group vibrations.

We have calculated the vibrational properties of **1** and **8** by DFT-B3LYP methods with 6-311+G** basis sets for all atoms using Gaussian03 routines.[24] For **1**, it has also been expedient to apply the same methods and basis sets within TURBOMOLE routines.[27] This led to some minor differences in the vibrational wavenumbers calculated by the two routines since the TURBOMOLE calculations, unlike the Gaussian ones, involved numerical and not analytical derivation. Full details of the calculated spectra of **1** and **8** can be found as Supporting Information.

The wavenumbers and intensities in IR absorption and Raman scattering that we have calculated for **1** are in broad, though not detailed, agreement with those reported previously.[4] Both **1** and **8** are expected to show IR and Raman spectra dominated by the high intensity in absorption or scattering of the ν(C−H) modes (calculated to lie between 3000 and 3130 cm^{-1}) and the breathing and deformation modes of the C_5Me_5 ligands (1400−1600 cm^{-1}). At wavenumbers below 1000 cm^{-1}, our calculations are consistent with the earlier ones[4] in predicting (a) distinctive, intense Raman scattering near 590, 380, and 110 cm^{-1} and (b) an intense IR absorption near 320 cm^{-1}, with a weaker feature at about 590 cm^{-1}, all arising from vibrational modes in which there is motion of the Zn atoms to a greater or lesser degree. Here we focus on the low-wavenumber region of both sets of spectra (drawing specifically on the results of the TURBOMOLE calculations for **1**) and on the identification of modes involving significant motion of the metal atoms, with particular emphasis on the Zn−Zn stretching coordinate of **1**.

The calculations identify no less than four distinctive Raman-active modes (all a_1') and three IR-active modes (all a_2'') occurring at wavenumbers <1000 cm^{-1}. The a_1' modes are predicted to occur at 593, 382, 229, and 107 cm^{-1}, the a_2'' modes at 591, 318, and 158 cm^{-1}. There can be little doubt then that the Raman bands observed at 590.8, 373.6, 236.0, and 130.7 cm^{-1} correspond to the four a_1' fundamentals and that the IR absorptions of the solid observed at 586.8 and 320.6 cm^{-1} correspond to the two higher energy a_2'' fundamentals; any sight

TABLE 3: Symmetry Coordinates Describing the a_1' and a_2'' Vibrational Fundamentals of $(\eta^5\text{-}C_5Me_5)_2Zn_2$[a]

a_1':

$S_1 = \Delta r(Zn-C_1) + \Delta r(Zn-C_2) + \Delta r(Zn-C_3) + \Delta r(Zn-C_4) + \Delta r(Zn-C_5) + \Delta r(Zn'-C'_1) + \Delta r(Zn'-C'_2) + \Delta r(Zn'-C'_3) + \Delta r(Zn'-C'_4) + \Delta r(Zn'-C'_5)$

$S_2 = \Delta r(C_1-C_{1a}) + \Delta r(C_2-C_{2a}) + \Delta r(C_3-C_{3a}) + \Delta r(C_4-C_{4a}) + \Delta r(C_5-C_{5a}) + \Delta r(C'_1-C'_{1a}) + \Delta r(C'_2-C'_{2a}) + \Delta r(C'_3-C'_{3a}) + \Delta r(C'_4-C'_{4a}) + \Delta r(C'_5-C'_{5a})$

$S_3 = \Delta r(C_{1a}-H_{1a}) + \Delta r(C_{2a}-H_{2a}) + \Delta r(C_{3a}-H_{3a}) + \Delta r(C_{4a}-H_{4a}) + \Delta r(C_{5a}-H_{5a}) + \Delta r(C'_{1a}-H'_{1a}) + \Delta r(C'_{2a}-H'_{2a}) + \Delta r(C'_{3a}-H'_{3a}) + \Delta r(C'_{4a}-H'_{4a}) + \Delta r(C'_{5a}-H'_{5a})$

$S_4 = \Delta r(C_{1a}-H_{1b}) + \Delta r(C_{2a}-H_{2b}) + \Delta r(C_{3a}-H_{3b}) + \Delta r(C_{4a}-H_{4b}) + \Delta r(C_{5a}-H_{5b}) + \Delta r(C_{1a}-H_{1c}) + \Delta r(C_{2a}-H_{2c}) + \Delta r(C_{3a}-H_{3c}) + \Delta r(C_{4a}-H_{4c}) + \Delta r(C_{5a}-H_{5c}) + \Delta r(C'_{1a}-H'_{1b}) + \Delta r(C'_{2a}-H'_{2b}) + \Delta r(C'_{3a}-H'_{3b}) + \Delta r(C'_{4a}-H'_{4b}) + \Delta r(C'_{5a}-H'_{5b}) + \Delta r(C'_{1a}-H'_{1c}) + \Delta r(C'_{2a}-H'_{2c}) + \Delta r(C'_{3a}-H'_{3c}) + \Delta r(C'_{4a}-H'_{4c}) + \Delta r(C'_{5a}-H'_{5c})$

$S_5 = \Delta r(Zn-Zn')$

$S_6 = \Delta r(C_1-C_2) + \Delta r(C_2-C_3) + \Delta r(C_3-C_4) + \Delta r(C_4-C_5) + \Delta r(C_1-C_5) + \Delta r(C'_1-C'_2) + \Delta r(C'_2-C'_3) + \Delta r(C'_3-C'_4) + \Delta r(C'_4-C'_5) + \Delta r(C'_1-C'_5)$

$S_7 = \Delta\angle(Zn-C_1-C_{1a}) + \Delta\angle(Zn-C_2-C_{2a}) + \Delta\angle(Zn-C_3-C_{3a}) + \Delta\angle(Zn-C_4-C_{4a}) + \Delta\angle(Zn-C_5-C_{5a}) + \Delta\angle(Zn'-C'_1-C'_{1a}) + \Delta\angle(Zn'-C'_2-C'_{2a}) + \Delta\angle(Zn'-C'_3-C'_{3a}) + \Delta\angle(Zn'-C'_4-C'_{4a}) + \Delta\angle(Zn'-C'_5-C'_{5a})$

$S_8 = \Delta\angle(C_1-C_{1a}-H_{1a}) + \Delta\angle(C_2-C_{2a}-H_{2a}) + \Delta\angle(C_3-C_{3a}-H_{3a}) + \Delta\angle(C_4-C_{4a}-H_{4a}) + \Delta\angle(C_5-C_{5a}-H_{5a}) + \Delta\angle(C'_1-C'_{1a}-H'_{1a}) + \Delta\angle(C'_2-C'_{2a}-H'_{2a}) + \Delta\angle(C'_3-C'_{3a}-H'_{3a}) + \Delta\angle(C'_4-C'_{4a}-H'_{4a}) + \Delta\angle(C'_5-C'_{5a}-H'_{5a})$

$S_9 = \Delta\angle(C_1-C_{1a}-H_{1b}) + \Delta\angle(C_2-C_{2a}-H_{2b}) + \Delta\angle(C_3-C_{3a}-H_{3b}) + \Delta\angle(C_4-C_{4a}-H_{4b}) + \Delta\angle(C_5-C_{5a}-H_{5b}) + \Delta\angle(C'_1-C'_{1a}-H'_{1b}) + \Delta\angle(C'_2-C'_{2a}-H'_{2b}) + \Delta\angle(C'_3-C'_{3a}-H'_{3b}) + \Delta\angle(C'_4-C'_{4a}-H'_{4b}) + \Delta\angle(C'_5-C'_{5a}-H'_{5b}) + \Delta\angle(C_1-C_{1a}-H_{1c}) + \Delta\angle(C_2-C_{2a}-H_{2c}) + \Delta\angle(C_3-C_{3a}-H_{3c}) + \Delta\angle(C_4-C_{4a}-H_{4c}) + \Delta\angle(C_5-C_{5a}-H_{5c}) + \Delta\angle(C'_1-C'_{1a}-H'_{1c}) + \Delta\angle(C'_2-C'_{2a}-H'_{2c}) + \Delta\angle(C'_3-C'_{3a}-H'_{3c}) + \Delta\angle(C'_4-C'_{4a}-H'_{4c}) + \Delta\angle(C'_5-C'_{5a}-H'_{5c})$

$S_{10} = \Delta\angle(H_{1b}-C_{1a}-H_{1c}) + \Delta\angle(H_{2b}-C_{2a}-H_{2c}) + \Delta\angle(H_{3b}-C_{3a}-H_{3c}) + \Delta\angle(H_{4b}-C_{4a}-H_{4c}) + \Delta\angle(H_{5b}-C_{5a}-H_{5c}) + \Delta\angle(H'_{1b}-C'_{1a}-H'_{1c}) + \Delta\angle(H'_{2b}-C'_{2a}-H'_{2c}) + \Delta\angle(H'_{3b}-C'_{3a}-H'_{3c}) + \Delta\angle(H'_{4b}-C'_{4a}-H'_{4c}) + \Delta\angle(H'_{5b}-C'_{5a}-H'_{5c})$

a_2'':

$S_{11} = \Delta r(Zn-C_1) + \Delta r(Zn-C_2) + \Delta r(Zn-C_3) + \Delta r(Zn-C_4) + \Delta r(Zn-C_5) - \Delta r(Zn'-C'_1) - \Delta r(Zn'-C'_2) - \Delta r(Zn'-C'_3) - \Delta r(Zn'-C'_4) - \Delta r(Zn'-C'_5)$

$S_{12} = \Delta r(C_1-C_{1a}) + \Delta r(C_2-C_{2a}) + \Delta r(C_3-C_{3a}) + \Delta r(C_4-C_{4a}) + \Delta r(C_5-C_{5a}) - \Delta r(C'_1-C'_{1a}) - \Delta r(C'_2-C'_{2a}) - \Delta r(C'_3-C'_{3a}) - \Delta r(C'_4-C'_{4a}) - \Delta r(C'_5-C'_{5a})$

$S_{13} = \Delta r(C_{1a}-H_{1a}) + \Delta r(C_{2a}-H_{2a}) + \Delta r(C_{3a}-H_{3a}) + \Delta r(C_{4a}-H_{4a}) + \Delta r(C_{5a}-H_{5a}) - \Delta r(C'_{1a}-H'_{1a}) - \Delta r(C'_{2a}-H'_{2a}) - \Delta r(C'_{3a}-H'_{3a}) - \Delta r(C'_{4a}-H'_{4a}) - \Delta r(C'_{5a}-H'_{5a})$

$S_{14} = \Delta r(C_{1a}-H_{1b}) + \Delta r(C_{2a}-H_{2b}) + \Delta r(C_{3a}-H_{3b}) + \Delta r(C_{4a}-H_{4b}) + \Delta r(C_{5a}-H_{5b}) + \Delta r(C_{1a}-H_{1c}) + \Delta r(C_{2a}-H_{2c}) + \Delta r(C_{3a}-H_{3c}) + \Delta r(C_{4a}-H_{4c}) + \Delta r(C_{5a}-H_{5c}) - \Delta r(C'_{1a}-H'_{1b}) - \Delta r(C'_{2a}-H'_{2b}) - \Delta r(C'_{3a}-H'_{3b}) - \Delta r(C'_{4a}-H'_{4b}) - \Delta r(C'_{5a}-H'_{5b}) - \Delta r(C'_{1a}-H'_{1c}) - \Delta r(C'_{2a}-H'_{2c}) - \Delta r(C'_{3a}-H'_{3c}) - \Delta r(C'_{4a}-H'_{4c}) - \Delta r(C'_{5a}-H'_{5c})$

$S_{15} = \Delta r(C_1-C_2) + \Delta r(C_2-C_3) + \Delta r(C_3-C_4) + \Delta r(C_4-C_5) + \Delta r(C_1-C_5) - \Delta r(C'_1-C'_2) - \Delta r(C'_2-C'_3) - \Delta r(C'_3-C'_4) - \Delta r(C'_4-C'_5) - \Delta r(C'_1-C'_5)$

$S_{16} = \Delta\angle(Zn-C_1-C_{1a}) + \Delta\angle(Zn-C_2-C_{2a}) + \Delta\angle(Zn-C_3-C_{3a}) + \Delta\angle(Zn-C_4-C_{4a}) + \Delta\angle(Zn-C_5-C_{5a}) - \Delta\angle(Zn'-C'_1-C'_{1a}) - \Delta\angle(Zn'-C'_2-C'_{2a}) - \Delta\angle(Zn'-C'_3-C'_{3a}) - \Delta\angle(Zn'-C'_4-C'_{4a}) - \Delta\angle(Zn'-C'_5-C'_{5a})$

$S_{17} = \Delta\angle(C_1-C_{1a}-H_{1a}) + \Delta\angle(C_2-C_{2a}-H_{2a}) + \Delta\angle(C_3-C_{3a}-H_{3a}) + \Delta\angle(C_4-C_{4a}-H_{4a}) + \Delta\angle(C_5-C_{5a}-H_{5a}) - \Delta\angle(C'_1-C'_{1a}-H'_{1a}) - \Delta\angle(C'_2-C'_{2a}-H'_{2a}) - \Delta\angle(C'_3-C'_{3a}-H'_{3a}) - \Delta\angle(C'_4-C'_{4a}-H'_{4a}) - \Delta\angle(C'_5-C'_{5a}-H'_{5a})$

$S_{18} = \Delta\angle(C_1-C_{1a}-H_{1b}) + \Delta\angle(C_2-C_{2a}-H_{2b}) + \Delta\angle(C_3-C_{3a}-H_{3b}) + \Delta\angle(C_4-C_{4a}-H_{4b}) + \Delta\angle(C_5-C_{5a}-H_{5b}) - \Delta\angle(C'_1-C'_{1a}-H'_{1b}) - \Delta\angle(C'_2-C'_{2a}-H'_{2b}) - \Delta\angle(C'_3-C'_{3a}-H'_{3b}) - \Delta\angle(C'_4-C'_{4a}-H'_{4b}) - \Delta\angle(C'_5-C'_{5a}-H'_{5b}) + \Delta\angle(C_1-C_{1a}-H_{1c}) + \Delta\angle(C_2-C_{2a}-H_{2c}) + \Delta\angle(C_3-C_{3a}-H_{3c}) + \Delta\angle(C_4-C_{4a}-H_{4c}) + \Delta\angle(C_5-C_{5a}-H_{5c}) - \Delta\angle(C'_1-C'_{1a}-H'_{1c}) - \Delta\angle(C'_2-C'_{2a}-H'_{2c}) - \Delta\angle(C'_3-C'_{3a}-H'_{3c}) - \Delta\angle(C'_4-C'_{4a}-H'_{4c}) - \Delta\angle(C'_5-C'_{5a}-H'_{5c})$

$S_{19} = \Delta\angle(H_{1b}-C_{1a}-H_{1c}) + \Delta\angle(H_{2b}-C_{2a}-H_{2c}) + \Delta\angle(H_{3b}-C_{3a}-H_{3c}) + \Delta\angle(H_{4b}-C_{4a}-H_{4c}) + \Delta\angle(H_{5b}-C_{5a}-H_{5c}) - \Delta\angle(H'_{1b}-C'_{1a}-H'_{1c}) - \Delta\angle(H'_{2b}-C'_{2a}-H'_{2c}) - \Delta\angle(H'_{3b}-C'_{3a}-H'_{3c}) - \Delta\angle(H'_{4b}-C'_{4a}-H'_{4c}) - \Delta\angle(H'_{5b}-C'_{5a}-H'_{5c})$

[a] Definition of the types of atoms: $(H_{na}H_{nb}H_{nc}C_{na})_{1...5}(C_n)_{1...5}Zn-Zn'(C'_n)_{1...5}(C'_{na}H'_{na}H'_{nb}H'_{nc})_{1...5}$. Primes denote symmetry-identical atoms related by the symmetry plane σ_h in the point group D_{5h}; n denotes symmetry-identical atoms related by the axis C_5. C_n is a C atom of the C_5 ring. C_{na} is a C atom of a methyl group. H_{na} is an H atom of a methyl group located in the mirror plane σ_v. H_{nb} and H_{nc} are symmetry-identical H atoms of a methyl group related by the mirror plane σ_v.

of the 158 cm^{-1} transition was denied by the absorption of the CsI host at wavenumbers lower than 200 cm^{-1}.

All the stretching vibrations in which a Zn atom is a bonding partner belong to either the a_1' (Raman-active) or the a_2'' (IR-active) representation of the D_{5h} $(\eta^5\text{-}C_5Me_5)_2Zn_2$ molecule. The symmetry-adapted internal coordinates, S_1-S_{19}, defined in Table 3 have therefore been devised in order to describe all 19 of the normal modes contained by these two irreducible representations. Switching from D_{5h} to C_1 symmetry to accommodate atoms of different mass requires a total of 150 symmetry coordinates; the remaining $150 - 19 = 131$ coordinates were automatically generated with the aid of the TURBOMOLE program suite.[30,33] With this set of symmetry coordinates, the force constant matrix was transformed from a framework based on Cartesian coordinates to one based on symmetry coordinates. Hence it has been possible to estimate potential energy distributions for the normal modes; the results for the a_1' and a_2'' modes occurring at wavenumbers below 1000 cm^{-1} are set out in Table 4. Here the calculated wavenumbers have been averaged to reflect the isotopic makeup of naturally occurring Zn atoms, and presented alongside are the wavenumber shifts expected to attend the switch from isotopically natural **1** to the $^{68}Zn_2$ isotopomer. The table also affords a comparison of these results with the experimental findings for solid **1**.

The appeal to symmetry coordinates provides an analytical description of the vibrational modes in terms of the coordinates Zn−Zn, Zn−C_{ring}, C_{ring}−C_{methyl}, C_5 ring-breathing, and ∠Zn−C_{ring}−C_{methyl}. The three a_2'' fundamentals at 591, 318, and 158 cm^{-1} are essentially out-of-phase versions of the totally symmetric a_1' fundamentals at 593, 382, and 229 cm^{-1}, respectively, with the one difference that the a_1' vibration at 382 cm^{-1} includes a significant measure of Zn−Zn stretching. In keeping with the results of earlier theoretical studies,[4] such stretching finds no expression as even the primary component of a single normal mode but contributes mainly and in varying degrees to the three a_1' modes at 382, 229, and 107 cm^{-1}. Only

TABLE 4: Potential Energy Distribution and ^{68}Zn Isotopic Splitting for the a_1' and a_2'' Vibrational Fundamentals of 1 Occurring at Wavenumbers <1000 cm^{-1}

theory[a]		experiment[a,b]					
ν	$\Delta\nu$	ν	$\Delta\nu$	irred. rep.	PED (%)	symmetry coordinate	character of motion[c]
107.4	−0.1	130.7	0.0	a_1'	42	S_1	ν(Zn−C_r)
					29	S_5	ν(Zn−Zn)
					27	S_7	δ(Zn−C_r−C_m)
228.6	−1.7	236.0	−3.6	a_1'	44	S_5	ν(Zn−Zn)
					53	S_7	δ(Zn−C_r−C_m)
381.8	−4.5	373.6	−4.2	a_1'	56	S_1	ν(Zn−C_r)
					27	S_5	ν(Zn−Zn)
					15	S_7	δ(Zn−C_r−C_m)
592.8	0.0	590.8	−1.8	a_1'	53	S_2	ν(C_r−C_m)
					46	S_6	C_5 breathing
157.8	−1.5	*d*	*d*	a_2''	35	S_{11}	ν(Zn−C_r)
					61	S_{16}	δ(Zn−C_r−C_m)
318.3	−1.8	320.6	−1.9	a_2''	63	S_{11}	ν(Zn−C_r)
					33	S_{16}	δ(Zn−C_r−C_m)
590.9	0.0	586.8	+0.9	a_2''	52	S_{12}	ν(C_r−C_m)
					46	S_{15}	C_5 breathing

[a] Results of TURBOMOLE calculations at the Gaussian B3LYP level with 6-311+G** basis sets for all atoms; wavenumbers derived numerically. Wavenumbers ν and $\Delta\nu$ in cm^{-1}. $\Delta\nu$ refers to the change in wavenumber on switching from isotopically natural **1** to the $^{68}Zn_2$ isotopomer. [b] Measurements made on the polycrystalline solid. [c] C_r = C atom of the C_5 ring; C_m = C atom of the methyl group. [d] Region obscured by absorption of the CsI pellet.

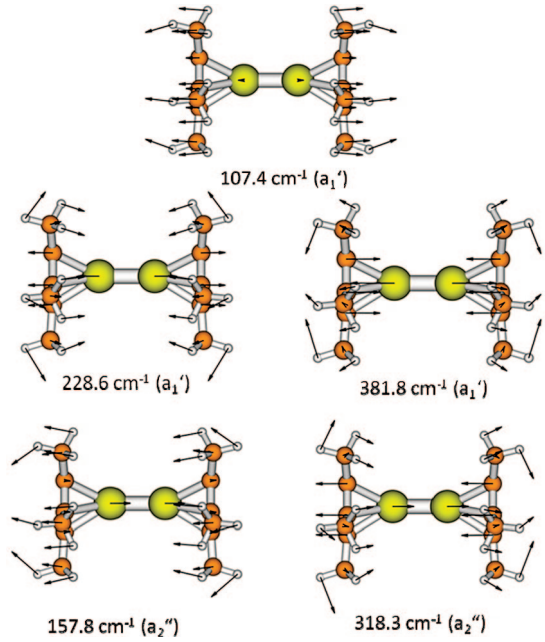

Figure 6. Raman-active (a_1') and IR-active (a_2'') modes involving significant motion of the Zn atoms in **1** and occurring at wavenumbers <400 cm^{-1}.

two of the IR-active a_2'' fundamentals involve significant motion of the metal atoms, namely, those calculated to occur at 318 and 158 cm^{-1}. These three a_1' and two a_2'' modes are depicted in Figure 6. Parts a and b of Figure 7 compare the simulated spectra of **1** and **8** in the region 0−900 cm^{-1}; how closely the calculations anticipate experiment may be judged by reference to the spectra measured for the polycrystalline solids.

Substitution of the natural mix of Zn isotopes by ^{68}Zn is predicted to produce shifts (a) of 0, −4.5, −1.7, and −0.1 cm^{-1} in the wavenumbers of the a_1' transitions originally centered at 593, 382, 229, and 107 cm^{-1}, respectively. For the a_2'' transitions at 591, 318, and 158 cm^{-1}, the corresponding shifts are 0, −1.8, and −1.2 cm^{-1}. The lack of response of the 107 cm^{-1} feature reflects partly its low wavenumber and partly the modest contribution of ν(Zn−Zn) to the vibration as a whole. The

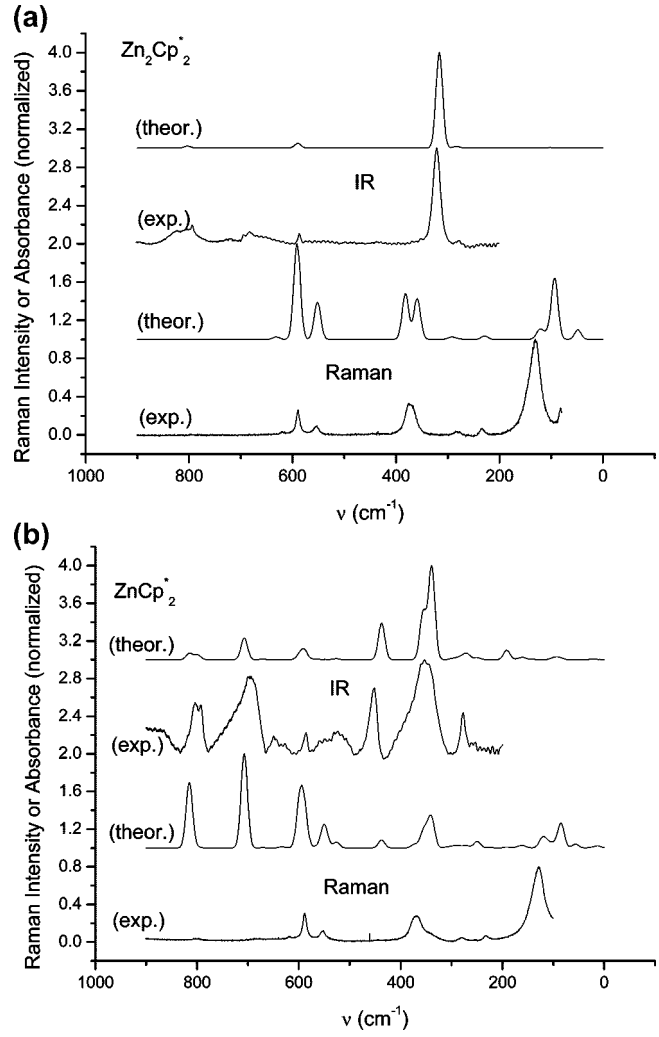

Figure 7. Simulated Raman and IR spectra of the molecules (a) **1** and (b) **8** in the region of 0−900 cm^{-1} compared with the spectra measured for the corresponding polycrystalline compounds.

predictions tally satisfactorily with the Raman and IR spectra measured for isotopically natural and ^{68}Zn-enriched samples of

1. The experimental measurements on the solid are necessarily limited by bandwidths at half-height, $\Delta\nu_{1/2,I}$, ranging between 7 and 26 cm^{-1} and by uncertainties of ± 1 cm^{-1}, at best, in the definition of the band centers. The comparative broadness of the Raman scattering at 373.6 cm^{-1} may well conceal an e_1' feature predicted to occur near 350 cm^{-1} but which is more or less insensitive to isotopic changes of the Zn atoms. With only one of the absorptions that could be observed (near 320 cm^{-1}) forecast to show a significant ^{68}Zn isotopic shift—and that not exceeding 2 cm^{-1}—the IR spectrum of solid **1** offers a less stringent test of theory than does the Raman spectrum. Nevertheless, the behavior of the absorptions at 586.8 and 320.6 cm^{-1}, with apparent shifts of +0.9 and −1.9 cm^{-1}, respectively, complies pleasingly well with the theoretically predicted shifts of 0 and −1.8 cm^{-1}. Even for matrix-isolated **1**, the IR absorption at 329.3 cm^{-1} (corresponding to that at 320.6 cm^{-1} for the solid) was characterized by $\Delta\nu_{1/2,I}$ = ca. 10 cm^{-1}, more than 3 times the maximum isotopic splitting to be expected for the $^{64}Zn_2$ and $^{68}Zn_2$ isotopomers of **1**; for practical reasons, the corresponding spectrum of the $^{68}Zn_2$ isotopomer could not be measured. The absorption at 329.3 cm^{-1} did display a contour suggestive of the quintet structure to be expected of a Zn_2 unit with a natural mix of Zn isotopes (see Figure 2 inset). However, the spacing between the components of the multiplet was about 2 cm^{-1} and the maximum spacing between what might be thought to correspond to the $^{64}Zn_2$ and $^{68}Zn_2$ components about 9 cm^{-1}. Accordingly, we are bound to conclude that the multiplet structure arises, at least in part, from the overlapping of two or more absorptions, possibly reflecting the trapping of molecules in different matrix sites.

From the transformation of the force constant matrix for **1** it was possible to extract an internal force constant f(Zn−Zn) = 1.42 mdyne $Å^{-1}$. This is substantially larger than the earlier estimate of 0.6 mdyne $Å^{-1}$ for the Zn_2^{2+} moiety formed in $ZnCl_2$ melts,[20] casting doubt on this result and on the precise nature of the vibration identified with the ν(Zn−Zn) vibration. According to the empirical relations linking force constant to internuclear distance developed by Badger and Herschbach and Laurie,[40] f(Zn−Zn) = 1.42 mdyne $Å^{-1}$ implies a Zn−Zn distance of 2.3−2.5 Å, in good agreement with the observed value of 2.305 Å; f(Zn−Zn) = 0.6 mdyne $Å^{-1}$ would imply a much longer distance, viz., 2.9−3.0 Å. Our value compares with f(M−M) = 1.11 and 1.68 mdyne $Å^{-1}$ for the cations M_2^{2+} where M = Cd and Hg, respectively.[17] Such a pattern, following the order Zn > Cd < Hg, is consistent with that found for other covalent bonds in which a group 12 metal atom is engaged, e.g., M^{II}−H[36] and M^{II}−C.[41] Bond lengths follow the reverse order, i.e., Zn < Cd > Hg, as found, for example, with the series of molecules Ar′MMAr′ [Ar′ = C_6H_3-2,6-(C_6H_3-2,6-$^iPr_2$)$_2$ and M = Zn, Cd, or Hg].[10c]

Our Gaussian calculations succeed also in simulating in a generally satisfactory way the Raman and IR spectra of the monozincocene (η^5-C_5Me_5)(η^1-C_5Me_5)Zn, **8**. As revealed in Figure 7b, the fit is by no means perfect. For example, the Raman scattering predicted to occur with significant intensity near 815 and 710 cm^{-1} is matched in the spectrum recorded for the polycrystalline solid by scattering at 805 and 685 cm^{-1}, but only as weak, broad bands (see Table 2). Such discrepancies are hardly surprising, however, for a complicated molecule of such low symmetry where it is hard to reproduce the precise makeup of the normal modes, particularly at lower wavenumbers. In any case, the calculations take no account of the effects of crystallization, with the change of symmetry from that of the isolated molecule to that of the unit cell, as well as the potentially complicating influence of intermolecular interactions (which may well lead to marked broadening of some bands). What is certain, though, is that both the calculated and measured spectra are significantly richer in detail than are those of **1**, in keeping with the relatively low symmetry of **8**, and the exact natures of the vibrations are correspondingly more difficult to define in simple terms. In distinct contrast with **1**, none of the Raman or IR bands of **8** shows a significant response when isotopically natural zinc is replaced by the single isotope ^{68}Zn. The greatest differences are otherwise apparent in the IR spectra of the two compounds. Hence, we note that the absorptions of solid **8** observed at 1274, 1005, 804, 697, 649, 524, 452, and 353 cm^{-1} (all with calculated counterparts) are not matched by corresponding features in the spectrum of solid **1**, whereas **8** does not display a strong absorption near 319 cm^{-1} analogous to that of **1**. The Raman spectrum of **8** contains bands at 1048.5 and 685 cm^{-1} that are not matched in the Raman spectrum of **1**; conversely, the Raman bands at 1030 and 555 cm^{-1} are characteristic of **1** but not of **8**. There are also differences of relative intensity, as revealed by a comparison of Figures 1 and 3. In view of the pronounced differences of structure, however, it comes as a considerable surprise that the spectra of the two compounds should have so much in common. For example, every one of the four distinctive a_1' modes in the Raman spectrum of **1** at 591, 374, 236, and 131 cm^{-1} is matched within less than 6 cm^{-1} by what appears to be a corresponding feature in the spectrum of **8**. Although the intense IR absorption of solid **1** due to the a_2'' mode at 321 cm^{-1} does not have a close match, its counterpart *could* be found in the 353 cm^{-1} absorption in the spectrum of **8**. The other distinctive a_2'' mode of **1** to be observed as a weak absorption at 587 cm^{-1} finds an obvious echo in a similarly weak absorption at 586 cm^{-1} in the IR spectrum of **8**. In short, it is the vibrations of the tethered C_5Me_5 ligands themselves, and neither the nuclearity of the metal center nor the mode of ligation, that dominate the Raman and IR spectra of these zincocene molecules. Only on close analysis of details such as ^{68}Zn isotopic shifts are the differences revealed.

4. Conclusions

The Raman and IR spectra measured for the solid, polycrystalline zincocenes (η^5-C_5Me_5)$_2$$Zn_2$, **1**, and ($\eta^5$-$C_5Me_5$)($\eta^1$-$C_5Me_5$)Zn, **8**, reflect only subtly the difference in structure of the two compounds and also the presence of the Zn−Zn bond in **1**. That the IR spectrum of each of the solids should resemble closely the spectrum of the vapor isolated in a solid Ar matrix at 12 K argues for the essentially molecular nature of the solid. Comparative simplicity, together with a significant lack of coincidences between the IR and Raman spectra at wavenumbers <1000 cm^{-1}, is consistent with a molecule of **1** enjoying a relatively high degree of symmetry (D_{5h}), and there is no hint of any feature suggestive of Zn−H−Zn bridging. Interpretation of the spectra has been aided not only by analogies with the spectra of related molecules, e.g., (η^5-C_5Me_5)$_2$Fe[34] but also by reference (i) to the effects of ^{68}Zn enrichment on the spectra of **1** and **8** and (ii) to the spectra simulated by DFT calculations at the B3LYP level. Hence it is made clear that motions of the C_5Me_5 ligands dominate the spectra of both compounds, irrespective of the mode of coordination, and that the Zn−Zn stretching motion of **1** features not as a single well-defined mode that can be identified with intense Raman scattering but to varying degrees in several normal modes having wavenumbers in the range of 100−400 cm^{-1}. An estimated stretching force constant, f(Zn−Zn), of 1.42 mdyne $Å^{-1}$ is more consistent with

the Zn−Zn bond length of 2.305 Å previously determined than is an earlier estimate of 0.6 mdyne $Å^{-1}$ for the Zn_2^{2+} moiety formed in $ZnCl_2$ melts.[20] Comparison with the M_2^{2+} cations (M = Cd or Hg)[17] then implies that the M−M stretching force constants follow the expected order Zn > Cd < Hg.

Acknowledgment. Financial support from the Spanish Ministerio de Educación y Ciencia (MEC) (project CTQ2007-62814 and Consolider-Ingenio 2010 CSD2007-00006) and the Junta de Andalucía (project FQM672) is gratefully acknowledged. I.R. thanks the Ministry of Education for a Research Grant, D.d.R. thanks the sixth framework program of the EU for an MC-OIF Fellowship, and A.R. thanks the MEC/Universidad de Sevilla for a Ramón y Cajal contract. R.K. thanks Sibylle Schneider for the preparation of the CsI pellets of the zincocenes.

Supporting Information Available: Results of TURBOMOLE and Gaussian quantum chemical calculations of the structures and vibrational spectra of $Zn_2Cp^*_2$ (**1**) and $ZnCp^*_2$ (**8**) and potential energy distributions of the a_1' and a_2'' vibrational fundamentals of $Zn_2Cp^*_2$ ($Cp^* = \eta^5$- or η^1-C_5Me_5); Tables S1−S6. This material is available free of charge via the Internet at http://pubs.acs.org.

References and Notes

(1) (a) Resa, I.; Carmona, E.; Gutierrez-Puebla, E.; Monge, A. *Science* **2004**, *305*, 1136–1138. (b) Del Río, D.; Galindo, A.; Resa, I.; Carmona, E. *Angew. Chem., Int. Ed.* **2005**, *44*, 1244–1247.

(2) (a) Parkin, G. A. *Science* **2004**, *305*, 1117–1118. (b) Schnepf, A.; Himmel, H.-J. *Angew. Chem., Int. Ed.* **2005**, *44*, 3006–3008.

(3) (a) Xie, Y.; Schaefer, H. F., III; King, R. B. *J. Am. Chem. Soc.* **2005**, *127*, 2818–2819. (b) Timoshkin, A. Y.; Schaefer, H. F. *Organometallics* **2005**, *24*, 3343–3345. (c) Xie, Z.-Z.; Fang, W.-H. *Chem. Phys. Lett.* **2005**, *404*, 212–216. (d) Kang, H. S. *J. Phys. Chem. A* **2005**, *109*, 4342–4351. (e) Liu, Z.-Z.; Tian, W. Q.; Feng, J.-K.; Zhang, G.; Li, W.-Q. *J. Mol. Struct. (THEOCHEM)* **2006**, *758*, 127–138. (f) Philpott, M. R.; Kawazoe, Y. *Chem. Phys.* **2006**, *327*, 283–290. (g) Pathak, B.; Pandian, S.; Hosmane, N.; Jemmis, E. D. *J. Am. Chem. Soc.* **2006**, *128*, 10915–10922. (h) Liu, Z.-Z.; Tian, W. Q.; Feng, J.-K.; Zhang, G.; Li, W.-K.; Cui, Y.-H.; Sun, Ch.-Ch. *Eur. J. Inorg. Chem.* **2006**, 2808–2818. (i) Velazquez, A.; Fernández, I.; Frenking, G.; Merino, G. *Organometallics* **2007**, *26*, 4731–4736.

(4) (a) Richardson, S. L.; Baruah, T.; Pederson, M. R. *Chem. Phys. Lett.* **2005**, *415*, 141–145. (b) Kress, J. W. *J. Phys. Chem. A* **2005**, *109*, 7757–7763.

(5) Grirrane, A.; Resa, I.; Rodriguez, A.; Carmona, E.; Alvarez, E.; Gutierrez-Puebla, E.; Monge, A.; Galindo, A.; del Río, D.; Andersen, R. A. *J. Am. Chem. Soc.* **2007**, *129*, 693–703.

(6) Wang, Y.; Quillian, B.; Wei, P.; Wang, H.; Yang, X.-J.; Xie, Y.; King, R. B.; Schleyer, P. V. R.; Schaefer, H. F., III; Robinson, G. H. *J. Am. Chem. Soc.* **2005**, *127*, 11944–11945.

(7) Fedushkin, I. L.; Skatova, A. A.; Ketkov, S. Y.; Eremenko, O. V.; Piskunov, A. V.; Fukin, G. K. *Angew. Chem., Int. Ed.* **2007**, *46*, 4302–4305.

(8) Yang, X.-J.; Yu, J.; Liu, Y.; Xie, Y.; Schaefer, H. F.; Liang, Y.; Wu, B. *Chem. Commun.* **2007**, 2363–2365.

(9) Tsai, Y.-C.; Lu, D.-Y.; Lin, Y.-M.; Hwang, J.-K.; Yu, J.-S. K. *Chem. Commun.* **2007**, 4125–4127.

(10) (a) Zhu, Z.; Wright, R. J.; Olmstead, M. M.; Rivard, E.; Brynda, M.; Power, P. P. *Angew. Chem., Int. Ed.* **2006**, *45*, 5807–5810. (b) Zhu, Z.; Fischer, R. C.; Fettinger, J. C.; Rivard, E.; Brynda, M.; Power, P. P. *J. Am. Chem. Soc.* **2006**, *128*, 15068. (c) Zhu, Z.; Brynda, M.; Wright, R. J.; Fischer, R. C.; Merrill, W. A.; Rivard, E.; Wolf, R.; Fettinger, J. C.; Olmstead, M. W.; Power, P. P. *J. Am. Chem. Soc.* **2007**, *129*, 10847–10857.

(11) Green, S. P.; Jones, C.; Stasch, A. *Science* **2007**, *318*, 1754.

(12) Van der Maelen, J. F.; Gutiérrez-Puebla, E.; Monge, A.; García-Granda, S.; Resa, I.; Carmona, E.; Fernández-Díaz, M. T.; McIntyre, G. J.; Pattison, P.; Weber, H.-P. *Acta Crystallogr.* **2007**, *B63*, 862.

(13) Aldridge, S.; Downs, A. J. *Chem. Rev.* **2001**, *101*, 3305–3365.

(14) Hao, H.; Cui, C.; Roesky, H. W.; Bai, G.; Schmidt, H.-G.; Noltemeyer, M. *Chem. Commun.* **2001**, 1118–1119.

(15) See, for example: Taylor, M. J. *Metal-to-Metal Bonded States of the Main Group Elements*; Academic Press: London, U.K., 1975.

(16) Woodward, L. A. *Philos. Mag.* **1934**, *18*, 823–827.

(17) Corbett, J. D. *Inorg. Chem.* **1962**, *1*, 700–703.

(18) Himmel, H.-J.; Gaertner, B. *Chem.—Eur. J.* **2004**, *10*, 5936–5941.

(19) (a) Beamish, J. C.; Boardman, A.; Small, R. W. H.; Worrall, I. J. *Polyhedron* **1985**, *4*, 983–987. (b) Tuck, D. G. *Polyhedron* **1990**, *9*, 377–386. (c) Beamish, J. C.; Boardman, A.; Worrall, I. J. *Polyhedron* **1991**, *10*, 95–99.

(20) Kerridge, D. H.; Tariq, S. A. *J. Chem. Soc. A* **1967**, 1122–1125.

(21) Fischer, B.; Wijkens, P.; Boersma, J.; van Koten, G.; Smeets, W. J. J.; Spek, A. L.; Budzelaar, P. H. M. *J. Organomet. Chem.* **1989**, *376*, 223–233.

(22) Blom, R.; Boersma, J.; Budzelaar, P. H. M.; Fischer, B.; Haaland, A.; Volden, H. V.; Weidlein, W. *Acta Chem. Scand., Ser. A* **1986**, *40*, 113–120.

(23) Macdonald, C. L. B.; Gorden, J. D.; Voigt, A.; Filipponi, S.; Cowley, A. H. *Dalton Trans.* **2008**, 1161–1176.

(24) See, for example: Zumbusch, A.; Schñockel, H. *J. Chem. Phys.* **1998**, *108*, 8092–8100.

(25) (a) Becke, A. D. *J. Chem. Phys.* **1993**, *98*, 5648–5652. (b) Lee, C.; Yang, W.; Parr, R. G. *Phys. Rev. B* **1988**, *37*, 785–789.

(26) Frisch, M. J.; Trucks, G. W.; Schlegel, H. B.; Scuseria, G. E.; Robb, M. A.; Cheeseman, J. R.; Montgomery, J. A., Jr.; Vreven, T.; Kudin, K. N.; Burant, J. C.; Millam, J. M.; Iyengar, S. S.; Tomasi, J. J.; Barone, V.; Mennucci, B.; Cossi, M.; Scalmani, G.; Rega, N.; Petersson, G. A.; Nakatsuji, H.; Hada, M.; Ehara, M.; Toyota, K.; Fukuda, R.; Hasegawa, J.; Ishida, M.; Nakajima, T.; Honda, Y.; Kitao, O.; Nakai, H.; Klene, M.; Li, X.; Knox, J. E.; Hratchian, H. P.; Cross, J. B.; Adamo, C.; Jaramillo, J.; Gomperts, R.; Stratmann, R. E.; Yazyev, O.; Austin, A. J.; Cammi, R.; Pomelli, C.; Ochterski, J. W.; Ayala, P. Y.; Morokuma, K.; Voth, A.; Salvador, P.; Dannenberg, J. J.; Zakrzewski, V. G.; Dapprich, S.; Daniels, A. D.; Strain, M. C.; Farkas, O.; Malick, D. K.; Rabuck, A. D.; Raghavachari, K.; Foresman, J. B.; Ortiz, J. V.; Cui, Q.; Baboul, A. G.; Clifford, S.; Cioslowski, J.; Stefanov, B. B.; Liu, G.; Liashenko, A.; Piskorz, P.; Komaromi, I.; Martin, R. L.; Fox, D. J.; Keith, T.; Al-Laham, M. A.; Peng, C. Y.; Nanayakkara, A.; Challacombe, M.; Gill, P. M. W.; Johnson, B.; Chen, W.; Wong, M. W.; Gonzalez, C.; Pople, J. A. Gaussian 03, revision C.02; Gaussian, Inc.: Wallingford, CT, 2004.

(27) Gorelsky, S. I. SWizard Program; York University: Toronto, Canada, 1998; http://www.sg-chem.net/.

(28) (a) DIAMOND: version 3.0; Bergerhoff, G.; Berndt, M.; Brandenburg, K. *J. Res. Natl. Inst. Stand. Technol.* **1996**, *101*, 221. (b) MOLDEN, version 3.9: Schaftenaar, G.; Noordik, J. H. *J. Comput.-Aided Mol. Des.* **2000**, *14*, 123.

(29) Ahlrichs, R.; Bär, M.; Häser, M.; Horn, H.; Kölmel, C. *Chem. Phys. Lett.* **1989**, *162*, 165–169.

(30) von Arnim, M.; Ahlrichs, R. *J. Chem. Phys.* **1999**, *111*, 9183–9190.

(31) (a) Vosko, S. H.; Wilk, L.; Nusair, M. *Can. J. Phys.* **1980**, *58*, 1200–1211. (b) Perdew, J. P. *Phys. Rev. B* **1986**, *33*, 8822−8824; **1986**, *34*, 7406. (c) Becke, A. D. *Phys. Rev. A* **1988**, *38*, 3098–3100. (d) Eichkorn, K.; Weigend, F.; Treutler, O.; Ahlrichs, R. *Theor. Chem. Acc.* **1997**, *97*, 119–124.

(32) Deglmann, P.; Furche, F.; Ahlrichs, R. *Chem. Phys. Lett.* **2002**, *362*, 511–518.

(33) Lide, D. R., Ed.-in-Chief *Handbook of Chemistry and Physics*, 88th ed.; CRC Press: Boca Raton, FL, 2007−2008.

(34) Duggan, D. M.; Hendrickson, D. N. *Inorg. Chem.* **1975**, *14*, 955–970.

(35) Howard, M. W.; Jayasooriya, U. A.; Kettle, S. F. A.; Powell, D. B.; Sheppard, N. *J. Chem. Soc., Chem. Commun.* **1979**, 18–19.

(36) Greene, T. M.; Brown, W.; Andrews, L.; Downs, A. J.; Chertihin, G. V.; Runeberg, N.; Pyykkö, P. *J. Phys. Chem.* **1995**, *99*, 7925–7934.

(37) (a) Pulham, C. R.; Downs, A. J.; Goode, M. J.; Rankin, D. W. H.; Robertson, H. E. *J. Am. Chem. Soc.* **1991**, *113*, 5149–5162. (b) Souter, P. F.; Andrews, L.; Downs, A. J.; Greene, T. M.; Ma, B.; Schaefer, H. F., III *J. Phys. Chem.* **1994**, *98*, 12824–12827.

(38) Baxter, P. L.; Downs, A. J.; Goode, M. J.; Rankin, D. W. H.; Robertson, H. E. *J. Chem. Soc., Dalton Trans.* **1990**, 2873–2881.

(39) James, D. W.; Parry, R. M.; Leong, W. H. *J. Raman Spectrosc.* **1978**, *7*, 71.

(40) Herschbach, D. R.; Laurie, V. W. *J. Chem. Phys.* **1961**, *35*, 458–463.

(41) See, for example: Gutowsky, H. S. *J. Chem. Phys.* **1949**, *17*, 128−138; *J. Am. Chem. Soc.* **1949**, *71*, 3194−3197.

JP805291E